Quantum confinement and magnetic-field effects on the electron *g* factor in GaAs–(Ga, Al)As cylindrical quantum dots

2009 J. Phys.: Condens. Matter 21 455302

(http://iopscience.iop.org/0953-8984/21/45/455302)

J. Phys.: Condens. Matter **21** (2009) 455302 (6pp) doi:10.1088/0953-8984/21/45/455302

Quantum confinement and magnetic-field effects on the electron g factor in GaAs–(Ga, Al)As cylindrical quantum dots

J R Mejía-Salazar[1], N Porras-Montenegro[1] and L E Oliveira[2,3]

[1] Departamento de Física, Universidad del Valle, AA 25360 Cali, Colombia
[2] Instituto de Física, Unicamp, CP 6165, Campinas, São Paulo 13083-970, Brazil
[3] Inmetro, Campus de Xerém, Duque de Caxias, Rio de Janeiro 25250-020, Brazil

Received 12 July 2009, in final form 22 September 2009
Published 21 October 2009
Online at stacks.iop.org/JPhysCM/21/455302

Abstract
We have performed a theoretical study of the quantum confinement (geometrical and barrier potential confinements) and axis-parallel applied magnetic-field effects on the conduction-electron effective Landé g factor in GaAs–(Ga, Al)As cylindrical quantum dots. Numerical calculations of the g factor are performed by using the Ogg–McCombe effective Hamiltonian—which includes non-parabolicity and anisotropy effects—for the conduction-band electrons. The quantum dot is assumed to consist of a finite-length cylinder of GaAs surrounded by a $Ga_{1-x}Al_xAs$ barrier. Theoretical results are given as functions of the Al concentration in the $Ga_{1-x}Al_xAs$ barrier, radius, lengths and applied magnetic fields. We have studied the competition between the quantum confinement and applied magnetic field, finding that in this type of heterostructure the geometrical confinement and Al concentration determine the behavior of the electron effective Landé $g_{\|}$ factor, as compared to the effect of the applied magnetic field. Present theoretical results are in good agreement with experimental reports in the limiting geometry of a quantum well, and with previous theoretical findings in the limiting case of a quantum well wire.

(Some figures in this article are in colour only in the electronic version)

1. Introduction

The conduction-electron effective Landé g factor in semiconductors and semiconductor heterostructures is one of the fundamental system properties that describes the magnitude of the Zeeman splitting of electronic states under applied magnetic fields. The g factor in semiconductor heterostructures differs from the free-electron g factor in vacuum, $g = 2.0023$, due to the spin–orbit interaction, confinement and non-parabolicity effects. As a result, there has been a number of experimental and theoretical works devoted to the understanding of the properties of the electron effective g factor in semiconductor heterostructures [1–14]. Due to the potential applications in the design and fabrication of spintronic and optoelectronic devices [15], such studies have been focused on semiconductor bulk materials [1, 2], quantum wells (QWs) [2–8], quantum well wires (QWWs) [9, 10], quantum dots (QDs) [11–13] and superlattices [14].

From the experimental point of view, for example, Oestreich and co-workers [2] studied the temperature-dependent GaAs electron g factor and observed an increasing Landé g factor as the temperature was increased. Hannak *et al* [2] measured the effective electron Landé factor in GaAs–$Ga_{1-x}Al_xAs$ QWs under in-plane applied magnetic fields. In addition, Le Jeune *et al* [4] studied the anisotropy of the electron Landé g factor in QWs whereas Malinowski and Harley [5] investigated the quantum confinement and built-in strain on the conduction-electron g factor in GaAs–$Ga_{0.65}Al_{0.35}As$ and strained GaAs–$Ga_{0.89}In_{0.11}As$ QWs. More recently, Hanson *et al* [16] measured the Zeeman splitting in a one-electron vertical QD as a function of the applied magnetic field and Köneman *et al* [17] has measured the anisotropy of spin splitting in GaAs–$Ga_{1-x}Al_xAs$ QDs by means of resonant tunneling spectroscopy. Theoretically, Kiselev *et al* [9] studied the Zeeman effect for electrons in one- and zero-dimensional semiconductor heterostructures in the framework of Kane's

model and investigated the properties of the electron g factor in QWWs and QDs in the absence of magnetic fields. Other works were devoted to an understanding of the effects of non-parabolicity and anisotropy on the conduction-electron effective Landé factor in GaAs–$Ga_{1-x}Al_xAs$ QWs [6, 7] and superlattices [14] under applied magnetic fields.

The investigations on the properties of the effective Landé g factor in QDs have been mainly carried out without the consideration of the aluminum concentration effects. In III–V bulk materials, the properties of the electron Landé g factor may be investigated within the $\mathbf{k}\cdot\mathbf{p}$ framework [1, 2]. According to this procedure, the behavior of the Landé g factor in each host material, as a function of the Al x concentration, is determined by the dependence of the fundamental gaps [18–23] and interband matrix elements as functions of the Al concentration [8]. In a semiconductor QD with zinc blende structure, the electron effective g factor must be studied by taking into account the anisotropy and non-parabolicity of the conduction band. In that respect, the effective Ogg–McCombe Hamiltonian [24] has been successfully used in order to obtain the electron effective Landé factor in GaAs–$Ga_{1-x}Al_xAs$ QWs [6, 7].

The aim of the present work is to study the role of the quantum confinement determined by the geometrical parameters of the structure and by the Al concentration, as well as the effects of an on-axis applied magnetic field on the conduction-electron g factor in GaAs–$Ga_{1-x}Al_xAs$ cylindrical QDs by taking into account the anisotropy and non-parabolicity of the conduction band. The present study is organized as follows. The theoretical procedure and a discussion of the effects of Al concentration on the g factor in each host material and on the GaAs–$Ga_{1-x}Al_xAs$ QD confining potential are given in section 2. Results and discussion are in section 3, and conclusions in section 4.

2. Theoretical framework

In the effective mass approximation and taking into account the non-parabolicity and anisotropy effects on the conduction band, the Ogg–McCombe effective Hamiltonian [24] for a conduction electron in a cylindrical GaAs–$Ga_{1-x}Al_xAs$ QD under an axis-parallel applied magnetic field, i.e. $\mathbf{B} = B\hat{\mathbf{z}}$, may be written as

$$\begin{aligned}\hat{H} = {} & \frac{\hbar^2}{2}\hat{\mathbf{K}}\frac{1}{m^*(\rho,z)}\hat{\mathbf{K}}\hat{\mathbf{I}} + \frac{1}{2}g(\rho,z)\mu_B B\hat{\sigma}_z + a_1\hat{\mathbf{K}}^4\hat{\mathbf{I}} + \frac{a_2}{l_B^4}\hat{\mathbf{I}} \\ & + a_3[\{\hat{K}_\rho^2,\hat{K}_\varphi^2\} + \{\hat{K}_\rho^2,\hat{K}_z^2\} + \{\hat{K}_\varphi^2,\hat{K}_z^2\}]\hat{\mathbf{I}} \\ & + a_4 B\hat{\mathbf{K}}^2\hat{\sigma}_z + a_5 B\{\hat{\vec{\sigma}}\cdot\hat{\mathbf{K}},\hat{K}_z\hat{\mathbf{I}}\} + a_6 B\hat{\sigma}_z\hat{K}_z^2 \\ & + V(\rho,z)\hat{\mathbf{I}}, \end{aligned} \tag{1}$$

where $\hat{\mathbf{K}} = -i\nabla + \frac{e}{\hbar c}\hat{\mathbf{A}}$, $\hat{\mathbf{I}}$ is the 2×2 unit matrix, μ_B is the Bohr magneton, $l_B = \sqrt{\frac{\hbar c}{eB}}$ is the Landau length, $\hat{\vec{\sigma}}$ is a vector for which the components are the Pauli matrices, $\{\hat{a},\hat{b}\} = \hat{a}\hat{b} + \hat{b}\hat{a}$ is the anticommutator between the $\hat{a}$ and $\hat{b}$ operators and the coefficients a_i ($i = 1,\ldots,6$) are constants which depend, in principle, on the Al concentration x. Due to the absence of experimental measurements on the behavior of the a_i coefficients as functions of x, we have taken the a_i values corresponding to bulk GaAs and obtained by a fitting with magnetospectroscopic measurements [25]. The cubic Dresselhaus spin–orbit interaction [26] can be neglected because its contribution to the effective g factor in GaAs–$Ga_{1-x}Al_xAs$ heterostructures may be shown to be quite minor [27, 28]. The position-dependent conduction-band effective mass $m^*(\rho,z)$ and Landé factor $g(\rho,z)$, together with the confinement potential $V(\rho,z)$, are considered to be dependent on the Al concentration x in each host material, as detailed below.

In the present work, we consider a QD modeled by a QW of width L in the z axis direction and a QWW of radius R in the (ρ,φ) plane. One may, therefore, choose to approximate the Hamiltonian (1) by

$$\hat{H} = \hat{H}(z) + \hat{H}(\rho,\varphi) + \hat{W}(\rho,\varphi), \tag{2}$$

where

$$\hat{H}(z) = \hat{K}_z(\hat{\beta}^{\pm}\hat{K}_z) + \hat{K}_z^2(a_1\hat{K}_z^2) + \hat{U}^{\pm}, \tag{3}$$

$$\hat{\beta}^{\pm}(z) = \frac{\hbar^2}{2m^*(z)} \pm (a_4 + 2a_5 + a_6)B + \frac{2(a_1+a_3)}{l_B^2}, \tag{4}$$

$$\hat{U}^{\pm} = V(z) \pm \tfrac{1}{2}g(z)\mu_B B, \tag{5}$$

$$\hat{H}(\rho,\varphi) = \hat{K}_{\rho,\varphi}(\chi^{\pm}\hat{K}_{\rho,\varphi}) + \hat{K}_{\rho,\varphi}^2\left(\left(a_1 + \tfrac{1}{4}a_3\right)\hat{K}_{\rho,\varphi}^2\right) + \xi, \tag{6}$$

$$\hat{K}_{\rho,\varphi} = \hat{K}_\rho + \hat{K}_\varphi, \tag{7}$$

$$\xi_{W,B} = \frac{a_2 - 0.75a_3}{l_B^4} + V(\rho), \tag{8}$$

$$\chi_{W,B}^{\pm} = \frac{\hbar^2}{2m^*(\rho)} \pm a_4 B, \tag{9}$$

where the subindices W and B denote the values of the magnitudes in the well and barriers, respectively, and the signs $\pm$ denote the states with parallel and antiparallel spin projections along the magnetic-field direction. Moreover [28, 29]

$$\hat{W}(\rho,\varphi) = \begin{pmatrix} \hat{W}_{11} & 0 \\ 0 & \hat{W}_{22} \end{pmatrix}, \tag{10}$$

where

$$\hat{W}_{11} = -\frac{a_3}{2l_B^4}(\hat{a}^{\dagger 4} + \hat{a}^4), \tag{11}$$

$$\hat{W}_{22} = -\frac{a_3}{2l_B^4}(\hat{a}^{\dagger 4} + \hat{a}^4), \tag{12}$$

and the $\hat{a}^\dagger$ creation and $\hat{a}$ annihilation operators are defined as in previous work [28, 29]. Here, one should consider that, in bulk GaAs, it may be verified that, for B varying up to 30 T, $|a_3|/l_B^4 \approx 10^{-3}$–$10^{-2}$ meV, i.e. $\hat{W}$ only contributes with insignificant corrections to the energy levels. Therefore, we will not take into consideration effects of $\hat{W}$ in the present study.

Now, in order to solve equation (3), we follow Sabín del Valle *et al* [29] and obtain similar results as their equations (10), (11) and (12). On the other hand, in

order to tackle equation (6), it is well known [30] that the solutions should be the Kummer confluent F and U hypergeometric functions, and one should then solve the following transcendental equation, which may be obtained by assuming as valid the boundary condition for the solution for the parabolic (equation (6) with $a_i = 0$) Hamiltonian, i.e.

$$\frac{\frac{\mathrm{d}}{\mathrm{d}\epsilon}(\mathrm{e}^{-\epsilon/2}\epsilon^{l/2}F[-\alpha_W^{\pm};l+1;\epsilon])}{\mathrm{e}^{-\epsilon/2}\epsilon^{l/2}F[-\alpha_W^{\pm};l+1;\epsilon]} = \frac{\frac{\mathrm{d}}{\mathrm{d}\epsilon}(\mathrm{e}^{-\epsilon/2}\epsilon^{l/2}U[-\alpha_{\mathrm{B}}^{\pm};l+1;\epsilon])}{\mathrm{e}^{-\epsilon/2}\epsilon^{l/2}U[-\alpha_{\mathrm{B}}^{\pm};l+1;\epsilon]}, \tag{13}$$

where

$$\alpha_{W,B}^{\pm} = -\frac{\chi_{W,B}^{\pm}l_{\mathrm{B}}^2}{a_3+4a_1} - \sqrt{\left(\frac{\chi_{W,B}^{\pm}l_{\mathrm{B}}^2}{a_3+4a_1}\right)^2 + \frac{l_{\mathrm{B}}^4(E_\rho^{\pm}-\xi_{W,B})}{a_3+4a_1}} - \frac{1}{2}, \tag{14}$$

and $\epsilon = \frac{eB\rho^2}{2\hbar c}$ is evaluated at $\rho = R$, where R is the radius of the QWW.

The axis-parallel electron effective Landé g factor in GaAs–(Ga, Al)As heterostructures may, therefore, be defined as

$$g_{||}^{(0)} = \frac{E_0^+ - E_0^-}{\mu_{\mathrm{B}}B}, \tag{15}$$

where

$$E_0^{\pm} = E_{z,0}^{\pm} + E_{\rho,0}^{\pm}, \tag{16}$$

and E_0^+ and E_0^- are the ground-state energies associated with spin-up and spin-down, respectively. The electron effective $g_{||}^{(0)}$ factor, obtained from equation (15), depends on the Al concentration in the $Ga_{1-x}Al_xAs$ barriers, applied magnetic field and QD geometrical parameters.

2.1. Landé g factor and effective mass: dependence on the Al concentration

In order to compute the electron effective Landé g factor in GaAs–$Ga_{1-x}Al_xAs$ heterostructures from equation (15), one needs to know the dependence of both the g factor and effective mass on the Al concentration in each host material (cf equation (1)). In that respect, many low temperature experiments have confirmed the remarkable accuracy of $\mathbf{k}\cdot\mathbf{p}$ calculations [31] for the most common III–V compounds and alloys. Here, we consider the five-band $\mathbf{k}\cdot\mathbf{p}$ theory for the g factor and effective mass as follows:

$$\frac{g}{g_0} = 1 - \frac{\Pi^2}{3}\left(\frac{1}{E(\Gamma_6^{\mathrm{c}}-\Gamma_8^{\mathrm{v}})} - \frac{1}{E(\Gamma_6^{\mathrm{c}}-\Gamma_8^{\mathrm{v}})+\Delta_0}\right) - \frac{\Pi'^2}{3}\left(\frac{1}{E(\Gamma_7^{\mathrm{c}}-\Gamma_6^{\mathrm{c}})} - \frac{1}{E(\Gamma_8^{\mathrm{c}}-\Gamma_6^{\mathrm{c}})}\right) + C' + \delta_g, \tag{17}$$

$$\frac{m_0}{m^*} = 1 + \frac{\Pi^2}{3}\left(\frac{2}{E(\Gamma_6^{\mathrm{c}}-\Gamma_8^{\mathrm{v}})} + \frac{1}{E(\Gamma_6^{\mathrm{c}}-\Gamma_8^{\mathrm{v}})+\Delta_0}\right) - \frac{\Pi'^2}{3}\left(\frac{1}{E(\Gamma_7^{\mathrm{c}}-\Gamma_6^{\mathrm{c}})} + \frac{2}{E(\Gamma_8^{\mathrm{c}}-\Gamma_6^{\mathrm{c}})}\right) + C + \delta_m, \tag{18}$$

where $g_0 = 2.0023$ and m_0 are the free-electron Landé factor and free-electron mass, respectively, and $E(\Gamma_8^{\mathrm{v}}, \Gamma_6^{\mathrm{c}}, \Gamma_7^{\mathrm{c}}, \Gamma_8^{\mathrm{c}})$ and Δ_0 are the energies of the band extrema at the center of the Brillouin zone and the split-off energy of the Γ_7^{v} valence band,

Table 1. Parameters used in the present calculation.

$E(x)$	a (meV)	b (meV)	c (meV)
$E(\Gamma_6^{\mathrm{c}}-\Gamma_8^{\mathrm{v}})$	1519[a]	1360[a]	220[a]
$E(\Gamma_6^{\mathrm{c}}-\Gamma_8^{\mathrm{v}})+\Delta_0$	1849[b]	1294[b]	220[b]
Π^2	28 900[c,d]	−6290[e]	0[e]
Π'^2	7784[f]	0[g]	0[g]
$E(\Gamma_7^{\mathrm{c}}-\Gamma_6^{\mathrm{c}})$	4504[h]	0[i]	0[i]
$E(\Gamma_8^{\mathrm{c}}-\Gamma_6^{\mathrm{c}})$	4659[h]	0[i]	0[i]

[a] From [20]. [b] From [23].
[c] From [1]. [d] From [8].
[e] Obtained from a linear fitting of the g-factor values for bulk $Ga_{1-x}Al_xAs$, reported in [8]. [f] From [33].
[g] To our knowledge, there are no experimental measurements on the Al concentration dependence of the Π'^2 matrix element, so we have taken $b = 0$ and $c = 0$.
[h] From [34].
[i] The remote-band contributions to the electron Landé g factor and effective mass are taken into account in equation (20).

Table 2. Aluminum concentration (x) dependence of the remote-band contributions for the electron g factor and effective mass of bulk GaAs–$Ga_{1-x}Al_xAs$.

$\delta(x)$	δ_1	δ_2
δ_g	−0.276	0.232
δ_m	0.488	4.938

respectively. The contributions from higher bands are taken into account via the terms [1] $C' = -0.02$, $C = -2$ and [8] δ_g, δ_m. The energies appearing in equations (17) and (18) depend on the Al concentration x and we denote them as $E(x)$, assuming that

$$E(x) = a + bx + cx^2, \tag{19}$$

with the values of the parameters a, b and c, corresponding to $Ga_{1-x}Al_xAs$, displayed in table 1. The remote-band contributions to the electron Landé g factor and effective mass are also expected to be functions of the Al concentration. However, up to now we do not know of any experimental report on such dependences in $Ga_{1-x}Al_xAs$ bulk materials. We have, therefore, considered δ_g and δ_m in equations (17) and (18), respectively, according to the expressions by Reyes-Gómez *et al* [32]:

$$\delta(x) = \delta_1 x + \delta_2 x^2, \tag{20}$$

with the values of δ_1 and δ_2, reported in table 2 obtained by fitting the experimental results corresponding to the electron g factor [1] and effective mass [35].

2.2. GaAs–$Ga_{1-x}Al_xAs$ QD confining potential

The value of the aluminum concentration at the barriers may change the properties of the confining potential. As is well known, there exists a critical value x_{c} of the aluminum concentration at which $Ga_{1-x}Al_xAs$ changes from a direct gap to an indirect gap material (Γ–X crossover), and this value was found by Guzzi *et al* [21] as $x_{\mathrm{c}} = 0.385$. We have considered that the confining potential corresponds [6]

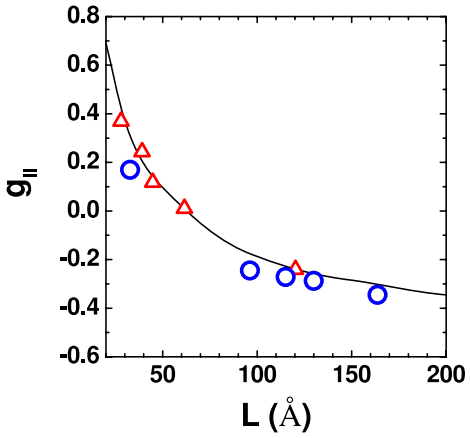

Figure 1. Electron effective Landé $g_{\parallel}$ factor for a radius $R = 300$ Å GaAs–$Ga_{0.65}Al_{0.35}As$ cylindrical QD as a function of the QD height L under an axis-parallel applied magnetic field $B = 0.1$ T. Present theoretical results are given as a full curve and experimental data, presented as open triangles and circles, are from measurements by Le Jeune *et al* [4] and Malinowski *et al* [5], respectively.

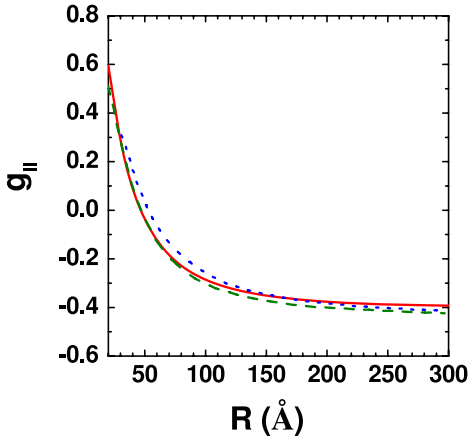

Figure 2. Electron effective Landé $g_{\parallel}$ factor for a GaAs–$Ga_{0.65}Al_{0.35}As$ cylindrical QD as a function of the QD radius under an axis-parallel applied magnetic field $B = 5$ T for an $L = 500$ Å QD height. The solid line corresponds to the present calculations, whereas the dotted curve is the theoretical result from Kiselev *et al* [9] and the dashed line is the calculation by López *et al* [10] for GaAs–$Ga_{0.65}Al_{0.35}As$ cylindrical QWWs.

to 60% of the gap difference between the two host materials, and the origin of energy is taken from the top of the GaAs valence band. In our calculations we have used the expression for the aluminum concentration-dependent confining potential following the relation by Li [23] for the energy gap in $Ga_{1-x}Al_xAs$, i.e.

$$V(x) = 816x + 132x^2. \tag{21}$$

3. Results and discussion

In what follows, we are concerned with a QD assumed to consist of a cylindrical pillbox of height L and radius R with GaAs surrounded by a $Ga_{1-x}Al_xAs$ barrier, under an axis-parallel applied magnetic field.

In order to assess the validity of our model for the study of cylindrical QDs, we should compare the present theoretical results with available experimental and theoretical results in the limiting cases of QWs, QWWs and bulk semiconductors. We have first calculated the electron Landé $g_{\parallel}$ factor in a GaAs–$Ga_{1-x}Al_xAs$ cylindrical QD by considering a very large QD radius, which is equivalent to having a QW, as a function of the height and applied magnetic fields at low temperatures. Theoretical results are displayed in figure 1 as a function of the QD height and compared with the experimental data by Le Jeune *et al* [4] and Malinowski *et al* [5] It is apparent from figure 1 that the present theoretical calculations are in very good agreement with the experimental measurements in this limiting case.

In figure 2, we present theoretical results for the electron $g_{\parallel}$ factor as a function of the radius by considering a large height of the pillbox, which is equivalent to considering a cylindrical QWW. These results compare quite well with numerical data reported by Kiselev *et al* [9] and López *et al* [10] in GaAs–$Ga_{0.65}Al_{0.35}As$ QWWs. In addition to the results presented in figures 1 and 2, we should note that, when both L and R QD geometrical parameters are very large, the value

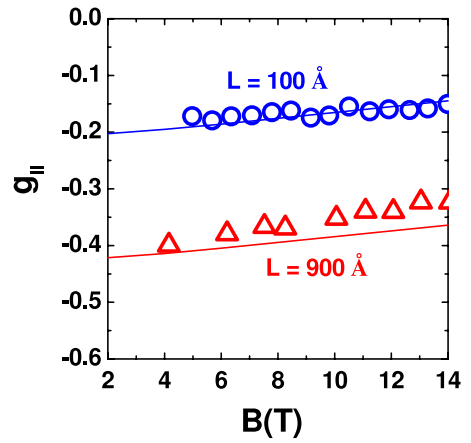

Figure 3. Electron effective $g_{\parallel}$ factor for a GaAs–$Ga_{0.7}Al_{0.3}As$ cylindrical QD as a function of the applied magnetic field for QD heights of $L = 100$ and 900 Å, and a QD radius of $R = 500$ Å. The solid line corresponds to the present calculations, and experimental data are given as open triangles and circles, from experimental measurements in QDs by Hanson *et al* [16] and Köneman *et al* [17], respectively.

of the $g_{\parallel}$ factor tends to the value in the bulk limit, which shows that the present QD model may be used to describe the behavior of the $g_{\parallel}$ factor in 1D, 2D and bulk systems. We can observe that the behavior of the electron effective $g_{\parallel}$ factor depends strongly on the geometry of the heterostructure, which is a consequence of the confining potential effect on the carrier wavefunction. When the geometrical parameters of the QD are increased, the wavefunction becomes more localized in the well material and, as a consequence, the effective electron $g_{\parallel}$ factor diminishes until reaching the -0.44 GaAs limiting value.

In figure 3 we display a comparison between the present theoretical calculations and experimental measurements of the effective electron $g_{\parallel}$ factor as a function of the applied

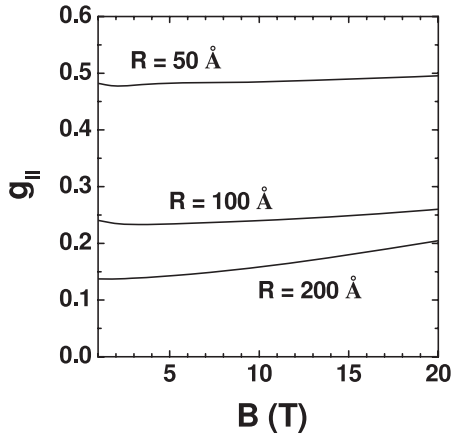

Figure 4. Electron effective Landé $g_{\parallel}$ factor for a GaAs–$Ga_{0.65}Al_{0.35}As$ cylindrical QD as a function of the applied magnetic field for a QD height of $L = 50$ Å, and three different QD radii.

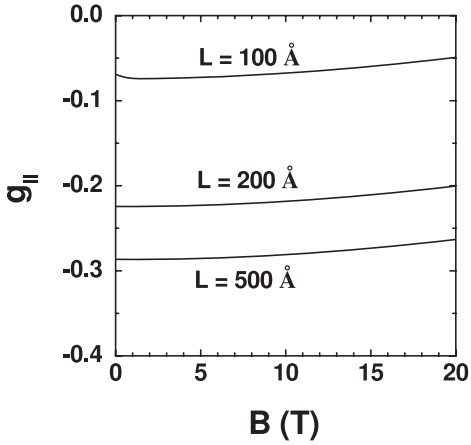

Figure 5. Electron effective Landé $g_{\parallel}$ factor for a GaAs–$Ga_{0.65}Al_{0.35}As$ cylindrical QD as a function of the applied magnetic field for a QD radius of $R = 100$ Å, and three different QD heights.

magnetic field. Calculations were carried out for $x = 0.3$, two different QD heights and by considering a large radius of the QD. Experimental data for GaAs–$Ga_{0.7}Al_{0.3}As$ QDs are from Hanson *et al* [16] and Köneman *et al* [17]. Despite the fact that the experimental data by Hanson *et al* [16] are for a magnetic field applied perpendicular to the QD axis, whereas present results are obtained for an on-axis applied magnetic field, one may note good agreement between theoretical results and experiment, which is due to the low anisotropy between $g_{\parallel}$ and $g_{\perp}$.

Figures 4 and 5 display the magnetic-field dependence of the effective electron $g_{\parallel}$ factor in GaAs–$Ga_{0.65}Al_{0.35}As$ QDs for $L = 50$ Å and different QD radii, and for $R = 100$ Å and different QD heights, respectively. It is apparent from figure 4 that the electron $g_{\parallel}$ factor essentially increases with the applied magnetic field, although this increment is lower for small QD radii as the geometric confinement determines the behavior of the $g_{\parallel}$ factor in contrast with the small magnetic-field confinement. For large QD radii, however, the $g_{\parallel}$ increment is mainly due to the magnetic-field confinement. For small QD radius, the electron wavefunction penetrates in the barrier regions and, therefore, the electron effective $g_{\parallel}$ factor is strongly influenced by the barrier properties. On the other hand, as the radius is increased, the cylindrical QD tends to the limiting geometry of the QW, in which case the radial confinement is dominated by the parabolic potential confinement due to the applied magnetic field. In contrast, from figure 5, one may note that the $g_{\parallel}$ factor increases with the applied magnetic field, with small slopes depending on the height of the pillbox.

The electron effective Landé $g_{\parallel}$ factor dependence on the aluminum concentration in a $Ga_{1-x}Al_xAs$ cylindrical quantum pillbox is displayed in figure 6 for different combinations of the geometrical parameters and applied magnetic fields. One may note that the Landé $g_{\parallel}$ factor increases with the aluminum concentration in the barrier material, although changes are less dramatic as the QD geometrical parameters are increased. On the other hand, one may note that the effect of the strength

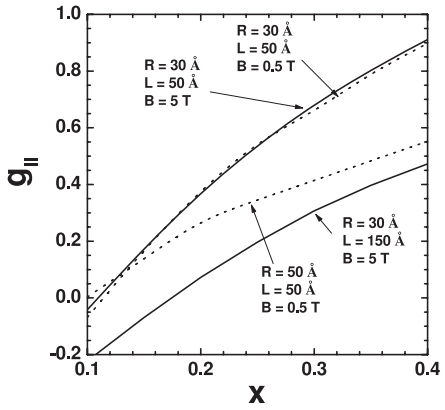

Figure 6. Electron effective Landé $g_{\parallel}$ factor for a GaAs–$Ga_{1-x}Al_xAs$ cylindrical QD as a function of the aluminum concentration x and for different combinations of applied magnetic fields, QD radii and QD heights.

of the applied magnetic field is less important for higher geometrical confinement. As discussed above, for small values of the geometrical parameters, the electron wavefunction has a larger penetration in the barrier regions, and therefore the effective $g_{\parallel}$ factor is strongly influenced by the barrier material properties.

We would like to emphasize that a realistic calculation of the effective Landé factor for semiconductor heterostructures must include the non-parabolic/anisotropic terms in the model Hamiltonian in order to obtain a quantitative understanding of experimental results, as shown in great detail via the Ogg–McCombe effective Hamiltonian [24] in figure 5 by López *et al* [10] and figure 4 by Reyes-Gómez *et al* [28]. Of course, non-parabolicity and anisotropic effects in the conduction band may also be taken into account through a calculation in which conduction, valence and higher band effects are considered within the same theoretical framework in a multi-band calculation [36].

4. Conclusions

In conclusion, we have performed a theoretical study of the effects of quantum confinement and axis-parallel applied magnetic fields on the conduction-electron effective Landé g factor in GaAs–$Ga_{1-x}Al_xAs$ cylindrical QDs. We have shown that the quantum confinement is determined by the geometrical parameters of the quantum pillbox, such as its radius, height and Al concentration, which essentially define the behavior of the electron effective Landé $g_{\|}$ factor. We have studied the competition between quantum confinement and applied magnetic field, and found that, in this type of heterostructure, the geometrical confinement and Al concentration determine the behavior of the electron effective $g_{\|}$ factor. The effect of the applied magnetic field, although weak in the regime of high geometrical confinement, is more apparent in the low confinement regime. Finally, the present theoretical treatment shows results that are in good agreement with experimental reports in the limiting geometry of a QW and with previous theoretical findings in the limiting case of a QWW.

Acknowledgments

The authors would like to thank both CENM and COLCIENCIAS from Colombia and the Brazilian agencies CNPq, FAPESP, and FAPERJ for partial financial support.

References

[1] Weisbuch C and Hermann C 1977 *Phys. Rev.* B **15** 816
Hermann C and Weisbuch C 1977 *Phys. Rev.* B **15** 823
[2] Oestreich M and Rühle W W 1995 *Phys. Rev. Lett.* **74** 2315
Hannak R M, Oestreich M, Heberle A P, Rühle W W and Kohler K 1995 *Solid State Commun.* **93** 313
Oestreich M, Hallstein S, Heberle A P, Eberl K, Bauser E and Rühle W W 1996 *Phys. Rev.* B **53** 7911
[3] Snelling M J, Flinn G P, Plaut A S, Harley R T, Tropper A C, Eccleston R and Phillips C C 1991 *Phys. Rev.* B **44** 11345
Heberle A P, Rühle W W and Ploog K 1994 *Phys. Rev. Lett.* **72** 3887
[4] Le Jeune P, Robart D, Marie X, Amand T, Brosseau M, Barrau J, Kalevcih V and Rodichev D 1997 *Semicond. Sci. Technol.* **12** 380
[5] Malinowski A and Harley R T 2000 *Phys. Rev.* B **62** 2051
[6] de Dios-Leyva M, Reyes-Gómez E, Perdomo-Leiva C A and Oliveira L E 2006 *Phys. Rev.* B **73** 085316
[7] de Dios-Leyva M, Porras-Montenegro N, Brandi H S and Oliveira L E 2006 *J. Appl. Phys.* **99** 104303
[8] Yugova I A, Greilic A, Yakovlev D R, Kiselev A A, Bayer M, Petrov V V, Dolgikh Yu K, Reuter D and Wieck A D 2007 *Phys. Rev.* B **75** 245302
[9] Kiselev A A, Ivchenko E L and Rössler U 1998 *Phys. Rev.* B **58** 16353
[10] López F E, Rodríguez B A, Reyes-Gómez E and Oliveira L E 2008 *J. Phys.: Condens. Matter* **20** 175204
[11] Pryor C E and Flatté M E 2006 *Phys. Rev. Lett.* **96** 026804
[12] Mejía-Salazar J R and Porras-Montenegro N 2008 *Microelectron. J.* **39** 1366
[13] Mayer Alegre T P, Hernández F G G, Pereira A L C and Medeiros-Ribeiro G 2006 *Phys. Rev. Lett.* **97** 236402
[14] Reyes-Gómez E, Perdomo-Leiva C A, de Dios-Leyva M and Oliveira L E 2006 *Phys. Rev.* B **74** 033314
[15] Kato Y K, Myers R C, Gossard A C and Awschalom D D 2004 *Science* **306** 1910
Zutic I, Fabian J and Das Sarma S 2004 *Rev. Mod. Phys.* **76** 323
Chen Z, Carter S G, Bratschitsch R, Dawson P and Cundiff S T 2007 *Nat. Phys.* **3** 265
[16] Hanson R, Witkamp B, Vandersypen L M K, Willems van Beveren L H, Elzerman J M and Kowenhoven L P 2003 *Phys. Rev. Lett.* **91** 196802
[17] Köneman J, Haug R J, Maude D K, Fal'ko V I and Altshuler B L 2005 *Phys. Rev. Lett.* **94** 226404
[18] Varshni Y P 1967 *Physica* **34** 149
[19] Viña L, Logothetidis S and Cardona M 1984 *Phys. Rev.* B **30** 1979
[20] Bosio C, Staehli J L, Guzzi M, Burri G and Logan R A 1988 *Phys. Rev.* B **38** 3263
[21] Guzzi M, Grilli E, Oggioni S, Staehli J L, Bosio C and Pavesi L 1992 *Phys. Rev.* B **45** 10951
[22] Grilli E, Guzzi M, Zamboni R and Pavesi L 1992 *Phys. Rev.* B **45**
[23] Li E H 2000 *Physica* E **5** 215
[24] Ogg N R 1966 *Proc. Phys. Soc. Lond.* **89** 431
McCombe B O 1969 *Phys. Rev.* **181** 1206
[25] Golubev V G, Ivanov-Omskĭi V I, Minervin I G, Osutin A V and Polyakov D G 1985 *Sov. Phys.—JETP* **61** 1214
[26] Dresselhaus G 1955 *Phys. Rev.* **100** 580
[27] Krich J J and Halperin B I 2007 *Phys. Rev. Lett.* **98** 226802
[28] Reyes-Gómez E, Porras-Montenegro N, Perdomo-Leiva C A, Brandi H S and Oliveira L E 2008 *J. Appl. Phys.* **104** 023704
[29] Sabín del Valle J, López-Gondar J and de Dios-Leyva M 1989 *Phys. Status Solidi* b **151** 127
[30] Rensink M E 1969 *Am. J. Phys.* **37** 900
Branis S V, Li G and Bajaj K K 1993 *Phys. Rev.* B **47** 1316
Li G, Branis S V and Bajaj K K 1993 *Phys. Rev.* B **47** 15375
[31] Roth L, Lax B and Zwerdling S 1959 *Phys. Rev.* **114** 90
Pfeffer P and Zawadzki W 1990 *Phys. Rev.* B **41** 1561
Mayer H and Rössler U 1991 *Phys. Rev.* B **44** 9048 and references therein
[32] Reyes-Gómez E, Raigoza N and Oliveira L E 2008 *Phys. Rev.* B **77** 115308
[33] Hübner J, Döhrmann S, Hägele D and Oestreich M 2009 *Phys. Rev.* B **79** 193307
[34] Lautenschlager P, Garriga M, Logothetidis S and Cardona M 1987 *Phys. Rev.* B **35** 9174
[35] Zachau M, Koch F, Weimann G and Schlapp W 1986 *Phys. Rev.* B **33** 8564
[36] de Andrada e Silva E A, La Rocca G C and Bassani F 1997 *Phys. Rev.* B **55** 16293
Prado S J, Trallero-Giner C, Alcalde A M, Lopez-Richard V and Marques G E 2004 *Phys. Rev.* B **69** 201310 (R) and references therein